Ecological Indicators 117 (2020) 106577

Contents lists available at ScienceDirect

Ecological Indicators

journal homepage: www.elsevier.com/locate/ecolind

Vegetation dynamics and its response to climate change during the past 2000 years along the Amur River Basin, Northeast China

Dongxue Han[a,b], Chuanyu Gao[a], Hanxiang Liu[c], Xiaofei Yu[a,d], Yunhui Li[a], Jinxin Cong[a], Guoping Wang[a,*]

[a] Key Laboratory of Wetland Ecology and Environment, Northeast Institute of Geography and Agroecology, Chinese Academy of Sciences, Changchun 130102, China
[b] University of Chinese Academy of Sciences, Beijing 100049, China
[c] Key Laboratory of Alpine Ecology, Institute of Tibetan Plateau Research, Chinese Academy of Sciences, Beijing 100101, China
[d] School of Environment, Northeast Normal University, Changchun 130117, China

ARTICLE INFO

Keywords:
Pollen
Anthropogenic disturbance
Amur River Basin
High latitudes
Peatland
Vegetation composition and climate reconstruction

ABSTRACT

The Amur River Basin is located in high latitudes, which is sensitive to the global climate change. However, only a few previous studies have tried to study the climate change in this region. To better understand the historical variation of vegetation and climate during the past 2000 years, we present a new palynological data from the Lesser Khingan Mountains, and compared the vegetation change along the Amur River Basin. It was possible to reconstruct climate based on vegetation composition before human disturbance. The results show that: the climate was moderately cold and humid during the 2000 to 700 cal yr BP, and the vegetation was mainly coniferous and broad-leaved mixed forest, and the abundance of Cyperaceae was relatively high. After that, the temperature and humidity declined, corresponding to the Little Ice Age. And the vegetation types also obviously changed that the conifers expanded, and the contents of broad-leaved trees and herbaceous Cyperaceae decreased. Since about 150 cal yr BP, the climate tended to be warm which belonged to Current Warm Period, and the main vegetation type was the secondary forests. The spread of the Han farming culture accompanied by the territorial expansion of the Tang Dynasty to the Sanjiang Plain at around 1300 cal yr BP caused human disturbance occurred earlier in the Sanjiang Plain than the Greater and Lesser Khingan Mountains. Additionally, the anthropogenic activities obviously intensified during the past hundred years along the Amur River Basin.

1. Introduction

Global climate change and its ecological effects have become the focus of the world, which have been listed as one of the important research contents in international research program of the Past Global Changes (PAGES) and Climate Variability and Predictability (CLIVAR) (IPCC, 2013; Zhao et al., 2015). Results have been showed that the climate become warming, especially in high latitudes, such as boreal and subarctic regions (Melles et al., 2019). There are abundant peatlands in boreal and subarctic regions which play a crucial part of global biogeochemical cycle (Yu et al., 2009, 2010; Xing et al., 2015; Yu et al., 2017; Zhang et al., 2018a). Global warming can lead to the variability of peatlands. Numerous studies have focused on the peatlands in boreal and subarctic regions, such as North America, Europe and Western Siberia (Borren et al., 2004; Cai and Yu, 2011; Schellekens et al., 2011; Lamentowicz et al., 2015). By contrast, there is little attention on northeastern Asia where the peatland was also widespread, especially in northeastern China.

The Holocene is the most recent geological epoch (Zhao et al., 2015), but the influence of human activities was increased over the last few millennia. Human activities and natural environment together resulted in the temporal and spatial changes of vegetation landscapes during the Holocene (Zhang et al., 2015c; Mackenzie et al., 2018). Precise reconstruction of vegetational and climatic history in the Holocene is necessary (Xiao et al., 2004). Palynological analysis is commonly applied to reconstruct historical variability of vegetation and climate as vegetation composition responds to climatic change. And pollen in sediments of peatlands could provide direct information on the composition of regional vegetation.

The Amur River Basin, on the border of China and Russia, is located in the transition zone between the eastern edge of temperate grassland and the southern margin of boreal forest in Eurasia where is the sensitive area of global climatic change. During the last century, the temperature has risen by 1.3 °C in the Amur River Basin which was

* Corresponding author.
E-mail address: wangguoping@neigae.ac.cn (G. Wang).

https://doi.org/10.1016/j.ecolind.2020.106577
Received 30 June 2019; Received in revised form 22 October 2019; Accepted 25 May 2020
Available online 07 June 2020

generally synchronous to the global climatic change (Novorotskii, 2007; Bazarova et al., 2011). Furthermore, the Amur River Basin has accumulated abundant peat, which provides high-quality archival records of past vegetation history. The relatively continuous accumulation of peat also provides a good geological record for the reconstruction of climatic changes in the region (Bazarova et al., 2008a; Wang et al., 2015; Zhang et al., 2016; Yu et al., 2017).

Previous studies of paleoclimate records in northeastern China mainly concentrated on Sanjiang Plain (Zhang et al., 2015a, b, 2018b; Wang et al., 2015; Cong et al., 2016), Songnen Plain (Mackenzie et al., 2018), Changbai Mountains (Hong et al., 2001; Li et al., 2011; Chu et al., 2014; Stebich et al., 2015), Hulun Lake (Wen et al., 2010a, b), Dali Lake (Wen et al., 2017), and Moon Lake (Wu et al., 2016). However, the study of high latitudes in the Amur River Basin is poor, it is necessary to understand the variability of vegetation and climate along the Amur River Basin.

For this study, based on accelerator mass spectroscopy (AMS) ^{14}C dating, palynological analysis and principal component analysis methods, we presented a new pollen record on variability of palaeovegetation and palaeoclimate during the last 2000 years from Youhao peatland (YH) in the Lesser Khingan Mountains, northeast China. Then we summarized the new data with previously published pollen data (Tuqiang peatland in the Greater Khingan Mountains and Honghe peatland in the Sanjiang Plain) along the Amur River Basin, and compared with adjacent regions in the Russian Far East. We hypothesized that there was a synchrony of vegetation change along the Amur River Basin during the late Holocene. The objectives of this study were (i) to demonstrate the variations of vegetation and climate along the Amur River Basin during the last 2000 years, (ii) to discuss how climate changes and/or anthropogenic activities impacted the peatland vegetation succession in the area.

2. Materials and methods

2.1. Study area and sampling

The study area is located in the south of the Amur River Basin in northeastern China (Fig. 1). The Amur River Basin (41°42′-53°33′ N, 115°25′-135°02′ E) is the largest river basin in northeast Asia, the area of basin is about 1.84 × 10^6 km^2. The total length of the Amur river is about 5498 km, which flows from the Mongolia steppes, through China and Russia, and ends at the Amur Liman and the Sea of Okhotsk where it empties into the Pacific Ocean (Dai et al., 2015; Yu et al., 2017; Bao et al., 2018). The topography of the basin is generally high in the west and low in the east. The west of the basin is mainly mountains and plateaus, deep in the interior of Asia away from the ocean, belongs to a temperate continental climate. The east and central parts of the basin are dominated by plains, with a temperate humid monsoon climate. The Amur River Basin is the northernmost edge of the global monsoon climate zone. The mean annual temperature (Tann) here ranges from −8 to 6 °C, the average temperature in January is about −28.5 °C, and the average temperature in July is about 19.5 °C, with a long, cold and dry winter from November to April and a short, hot and wet summer from June to August. The mean annual precipitation (Pann) amounts to 250–800 mm, > 80% of the rainfall occurred in May to September. The rainfall mainly focuses on the east coastal area, and gradually declines towards to the west of the basin (Yu et al., 2014; Yang et al., 2015).

The sampled sites were selected along the Amur River Basin in Heilongjiang Province, northeastern China, including Tuqiang peatland (TQ, 52°56′34.62″ N, 122°51′17.46″ E, altitude 481 m above sea level (a.s.l.) in the Greater Khingan Mountains, Youhao peatland (YH, 48°09′40.42″ N, 128°45′02.69″ E, 306 m a.s.l.) in the Lesser Khingan Mountains, and Honghe peatland (HE, 47°35.096′ N, 133°30.006′ E, 71 m a.s.l.) in the Sanjiang Plain (Fig. 1). TQ peatland is situated in a valley, the dominant vegetation are shrubs (*Ledum palustre*, *Vaccinium uliginosum*), sedges (*Eriophorum vaginatum*) and *Sphagnum*, surrounded by *Larix gmelinii* and *Betula platyphylla* forests (Han et al., 2019). YH peatland is located in valley, its dominant species are herbs (*Carex*, *Calamagrostis angustifolia*, *Sanguisorba*) and surrounded by *Betula platyphylla* forests. HE peatland is located at alluvial plain, the topography is roughly circular in shape with a diameter of ~2 km and a mean water depth of 0.5 m in summer. It is dominated by herbaceous vegetation in its low-lying areas and surrounded by deciduous broadleaved forests (Zhang et al., 2015b). There is no contemporary in-flowing and out-flowing river within the catchment of these three peatlands and hydrological condition is mainly controlled by precipitation. The Tann of YH peatland is about −0.7 °C, the Pann is about 600 mm, and the coefficient of humidity is 1.13 (Yang and Wang, 2002). Core YH with a thickness of 80 cm was collected using a Russia Peat Corer in November 2016. A stainless steel knife was used to slice the sediment samples of YH core continuously at 1-cm intervals from the top down to 50 cm, and at intervals of 5-cm between 50 and 80 cm in the field. All samples were packed into tagged sealed polyethylene plastic bags, subsequently taken back to the laboratory for storage at −20 °C prior to analysis (Xing et al., 2015; Liu et al., 2018; Zhang et al., 2018b). The detailed information (sampling, dating and pollen diagram) of TQ and HE cores could be seen in previous published articles (Han et al., 2019; Zhang et al., 2015).

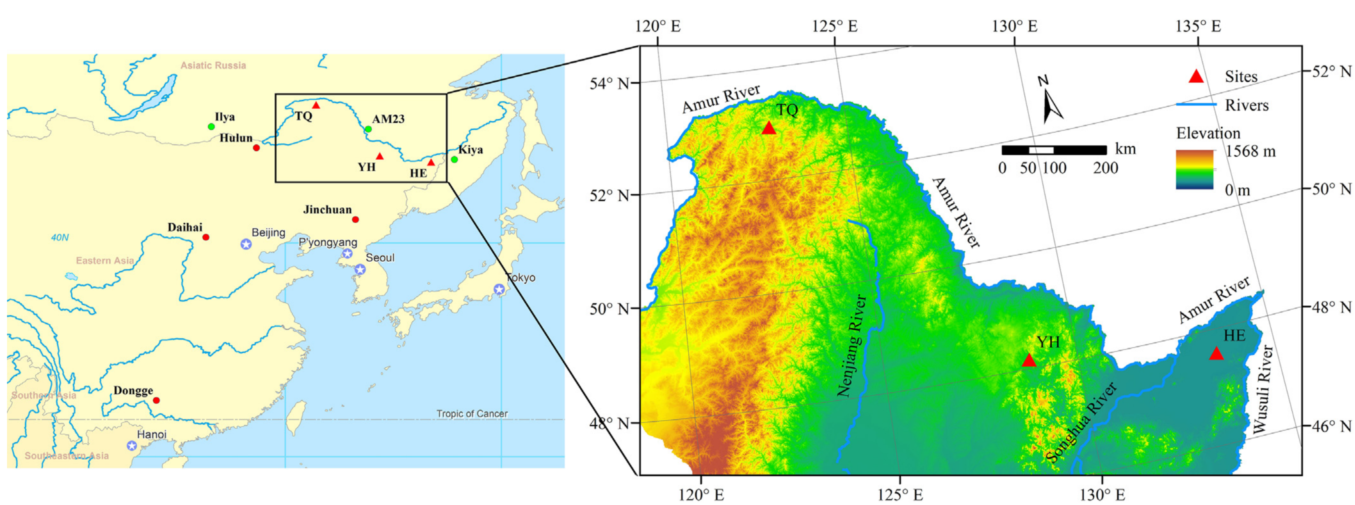

Fig. 1. Location of sites in Heilongjiang Province, northeast China (TQ: Tuqiang Peatland, YH: Youhao Peatland, HE: Honghe Peatland) along the Amur River Basin, and other paleoenvironmental proxy records discussed in the text. Green dots indicate sites in Russia (Ilya, AM23 and Kiya), red dots show sites in monsoon region in eastern China (Hulun Lake, Jinchuan Peatland, Daihai Lake and Dongge Cave).

2.2. Chronology

Four samples of YH core were dated using accelerator mass spectroscopy (AMS) ^{14}C radiocarbon dating in the State Key Laboratory of Loess and Quaternary Geology, Institute of Earth Environment, Chinese Academy of Sciences. Radiocarbon dating results were calibrated into calendar ages before present (0 yr BP = 1950 CE) using the Calib 7.04 software and IntCal 13 calibration curve (Reimer et al., 2013). The age-depth model was constructed using the 'Bacon' piecewise linear accumulation model (Blaauw and Christen, 2011) in R (R Core team, 2015). The obtained ages were used to calculate the sedimentation rates.

2.3. Pollen analysis

Palynological analysis followed the conventional methods (Fægri and Iversen, 1989), the preparation of pollen samples (1 g fresh sample) in the laboratory involved treatments with hydrochloric acid (HCl, 36%, 5 ml), sodium hydroxide (NaOH, 10%, 5 ml), hydrofluoric acid (HF, 40%, 5 ml), a 9:1 mixture (3 ml) of acetic anhydride and concentrated sulfuric acid, sieving with a 10-μm mesh screen in ultrasonic bath, and mounting in glycerine. A piece of *Lycopodium* spores (27,560 grains/tablet) were added to each sample as tracer at the beginning of the pre-treatment in order to estimate absolute pollen concentrations (grains/g). Pollen identification and counting were carried out under an Olympus BX-53 light microscope with 400 times magnification, with the aid of published pollen atlases by Wang et al. (1995) and Tang et al. (2016). More than 400 terrestrial pollen grains (423 pollen grains in average) were identified and counted per sample of YH core. The total sum of terrestrial pollen taxa identified in each sample was used as denominator when calculating pollen percentages, while the percentage of ferns spores was calculated based on the sum of terrestrial pollen plus ferns spores (Zhao et al., 2010). Pollen diagrams were drawn using the Tilia version 1.7.16 and pollen-assemblage zones were divided based on stratigraphically constrained cluster analysis (CONISS).

2.4. Numerical analyses

Numerical analyses were performed using pollen taxa which occurred in at least three samples with a percentage of > 3%. A total of 11 pollen taxa from YH core were selected and the analyses were carried out on the basis of the square-root transformed pollen percentage data using Canoco 4.5 (TerBraak and Smilauer, 2003). Detrended correspondence analysis (DCA) was used to determine whether linear or unimodal based techniques should be employed in the subsequent ordination analysis. The gradient length of the first axis was 0.639 standard deviation (SD) units, which was less than 2, showing that the data set had a mainly linear structure and suggesting use of the linear-based principal component analysis (PCA). Therefore, PCA analysis was performed to analyze the pollen assemblages in YH core using inter-species correlations and pollen percentages (Birks and Gordon, 1985; Herzschuh et al., 2006; Wen et al., 2010b; Chen et al., 2014; Zhao et al. 2015; Xu et al., 2016; Yao et al., 2017).

3. Results

3.1. ^{14}C dating of core YH

The chronology of YH core was based on four radiocarbon dates, the lowermost part of the YH core was dated to approximately 1750 cal yr BP (Fig. 2), the detail information including laboratory numbers, test materials and the calibrated ages were showed in Table 1.

3.2. Pollen assemblages of core YH

A total of 41 pollen and spore taxa were identified in 56 fossil sediment samples from the core YH, including 14 trees, 24 herbs and some Polypodiaceae, Ephedraceae and Trilete fern spores. Arboreal pollen mainly consisted of *Pinus* (6.7–24.6%) and *Betula* (9.3–23.6%); herbaceous pollen was mainly from Cyperaceae (21.5–52.7%), Poaceae (< 35 μm) (0.9–17.7%), *Artemisia* (3.5–8.0%), *Sanguisorba* (0.2–8.1%), *Thalictrum* (0.2–3.7%) and Chenopodiaceae (0.2–2.6%). Pollen concentrations ranged from 3.8×10^4 to 2.0×10^5 grains/g. The pollen diagram of core YH was divided into three zones based on the results of pollen assemblages and CONISS analysis (Fig. 3).

3.2.1. Zone 1 (depth range 80–28 cm): 1750–700 cal yr BP

The percentage of Cyperaceae up to 36.5–52.7%, which predominated throughout the pollen assemblages. The percentages of Poaceae (< 35 μm) and *Artemisia* reached 1.8–9.5% and 3.5–7.9%, respectively. At the depth of 34 cm, cereal Poaceae (> 35 μm) occurred. The herbs content ranged from 55.1 to 69.8%. Arborous species were mainly dominated by *Pinus* (8.0–19.6%) and *Betula* (10.8–23.6%), coniferous trees pollen percentages fluctuated from 10.1 to 23.5%, broad-leaved trees pollen percentages varied from 15.4 to 28.7%. Polypodiaceae spore percentages were 1.6–10.9%. Pollen concentrations were 4.7×10^4–1.9×10^5 grains/g. The sedimentation rate reached 0.5 mm/year.

3.2.2. Zone 2 (depth range 28–5 cm): 700–150 cal yr BP

Cyperaceae pollen (33.1–50.4%) was still dominant, though pollen content dropped compared with zone 1, Poaceae (< 35 μm) (0.9–10.8%) and *Artemisia* (3.7–8.0%) pollen contents increased. The content of herbs was 50.5–67.6%. *Pinus* pollen content (up to 7.0–24.6%) increased while *Betula* pollen content (9.3–21.6%) declined, coniferous and broad-leaved trees pollen content was 8.9–29.5% and 13.9–28.6%, respectively. Polypodiaceae spore content increased to 4.2–14.6%. Pollen concentrations dropped down to 3.8×10^4-1.5×10^5 grains/g. The sedimentation rate was 0.4 mm/year.

3.2.3. Zone 3 (depth range 5–0 cm): since around 150 cal yr BP

The proportion of Cyperaceae pollen (21.5–41.5%) decreased continuously, *Artemisia* (3.6–5.3%) decreased while Poaceae (< 35 μm) (up to 3.9–17.7%) increased. Besides, the proportion of human-companion plants, such as *Aster*, *Taraxacum*, Polygonaceae and Ranunculaceae increased. The percentage of herbs was between 42.5 and 66.5%. *Pinus* and *Betula* pollen proportions were 6.7–22.2% and 12.2–19.1%, respectively. Conifers pollen content was 10.0–27.1%, and broad-leaved trees pollen content was 17.8–40.3%. The proportion of Polypodiaceae dropped to 2.1–8.8%. Pollen concentrations varied from 4.9×10^4 to 2.0×10^5 grains/g. The sedimentation rate was minimum only 0.3 mm/year.

3.3. PCA analysis results of core YH

The PCA results based on 11 selected pollen taxa and the total number of samples were shown in Fig. 4. The first and second principal components captured 22.7% and 14.1%, respectively, altogether accounted for 36.8% of the total variance within fossil pollen assemblages. The 11 main pollen taxa were divided into four groups: (1) Poaceae (< 35 μm). (2) *Sanguisorba*, *Quercus* and Cyperaceae. (3) *Pinus*, *Picea* and *Abies*. (4) Polypodiaceae, *Artemisia*, *Betula*, *Alnus* and *Salix*. Three clusters of samples showed good correspondence with pollen assemblage zones, separated from each other clearly on the biplot of PCA scores along the first and the second axis: zone 1 (1750–700 cal yr BP) characterized by Cyperaceae and *Quercus*, zone 2 (700–150 cal yr BP) characterized by *Pinus*, *Picea*, *Abies* and Polypodiaceae, zone 3 (since about 150 cal yr BP) characterized by Poaceae (< 35 μm). As shown in Fig. 4, the PCA axis 1 separated the cold-tolerant *Pinus*, *Picea* and *Abies* on the left from the thermophilic *Betula* and *Alnus* on the right. On the other hand, the PCA axis 2 separated hygrophilic Cyperaceae, Poaceae (< 35 μm) and *Sanguisorba* above from the drought-tolerant *Artemisia* below. This implied that the PCA axis 1 mainly

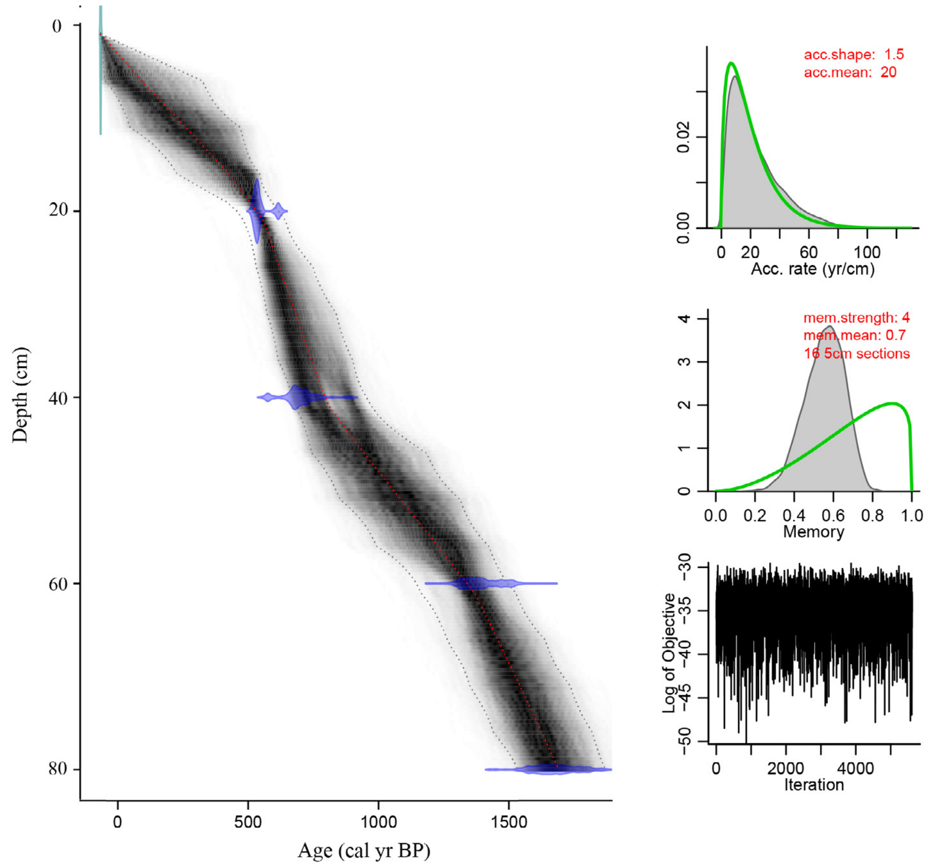

Fig. 2. The AMS ^{14}C bacon age-depth model of core YH.

Table 1
Calibrated Accelerator Mass Spectrometry (AMS) radiocarbon dates of YH core.

Depth (cm)	Lab No.	Dated material	AMS ^{14}C age (^{14}C yr BP)	Calibrated age (cal yr BP) (2σ range)
YH-20	Poz-93777	Bulk peat	495 ± 30	525 ± 24
YH-40	Poz-93809	Bulk peat	860 ± 30	747 ± 53
YH-60	Poz-93810	Bulk peat	1600 ± 30	1481 ± 69
YH-80	Poz-94117	Bulk peat	1800 ± 35	1755 ± 65

represented temperature changes: positive values indicated a warm climate, while negative values indicated a cold climate. PCA axis 2 reflected effective moisture changes: positive and negative values indicated wet and dry conditions, respectively.

4. Discussion

4.1. Climate change reflected by vegetation in YH peatland

The pollen assemblages of YH core revealed a detailed history of vegetation and climate changes in YH peatland in the late Holocene. During the period between 1750 and 700 cal yr BP, the peatland vegetation was predominated by herbaceous plants, mainly Cyperaceae with some Poaceae (< 35 μm), *Artemisia*, Chenopodiaceae, *Sanguisorba* and *Thalictrum* (Fig. 3). High content of Cyperaceae reflected high moisture levels (Yu et al., 2017). The pollen content of hygrophilous Cyperaceae was the highest in the whole YH core which reflected a relatively wet condition (Fig. 3), PCA axis 2 score curve also implied a wet climate (Fig. 5). The reconstructed precipitation records of Daihai Lake and Hulun Lake which based on pollen data also suggested a wet environment at the same period, and the stalagmite record from Dongge Cave exhibited a relatively intense East Asian Summer Monsoon (Fig. 5). The surrounding arboreal plants primarily consisted of *Pinus* and *Betula*, with a few *Picea*, *Abies*, *Alnus*, *Ulmus*, *Quercus* and *Salix*, suggesting a coniferous and broad-leaved mixed forest around the YH peatland. Yao et al. (2017) proposed that *Pinus* was indicative of low temperature climate. The proportions of *Pinus*, *Picea* and *Abies* which adapted to cold condition were relatively high (Fig. 3), suggesting a cold climate. PCA axis 1 score curve exhibited a cold condition, the reconstructed temperature curve (Tann) based on pollen data from Hulun Lake also marked a colder climate (Fig. 5, Wen et al., 2010a). So we inferred that the climate was relatively cold and wet between 1750 and 700 cal yr BP. It was noteworthy that at about 1050 cal yr BP, there was a peak value of PCA axis 1 score, the records of Hulun Lake and Jinchuan peatland also exhibited a relatively high temperature, which could correspond to the Medieval Warm Period (930–1240 CE, 1020–710 cal yr BP), afterwards, a cooling of climate took place (Fig. 5).

The interval from 700 to 150 cal yr BP, the pollen content of hygrophilous Cyperaceae reduced, while the Polypodiaceae spore content increased apparently and reached a maximum value (Fig. 3), denoting a decreased rainfall at this stage when compared with the previous period. The reduced scores of PCA axis 2 further marked a trend of dry condition, the Pann curve from Daihai Lake suggested a drier environment and the oxygen isotope proxy of Dongge Cave implied a declined intensity of East Asian Summer Monsoon (Fig. 5). The percentages of cold-tolerate *Pinus*, *Picea* and *Abies* species increased and reached the peak values in the entire YH core at around 300 cal yr BP, the content of broad-leaved trees (*Quercus*, *Juglans* and *Tilia*) decreased (Fig. 3), which revealed the expansion of needle forests and a cooling of the climate. The lower PCA axis 1 score still displayed the cold climate, though fluctuations existed (Fig. 5). This cold and dry event could correspond to the Little Ice Age (LIA), which formally defined as lasting from 1500 to 1850 CE (450–100 cal yr BP) (Lamb, 1972; Mann et al.,

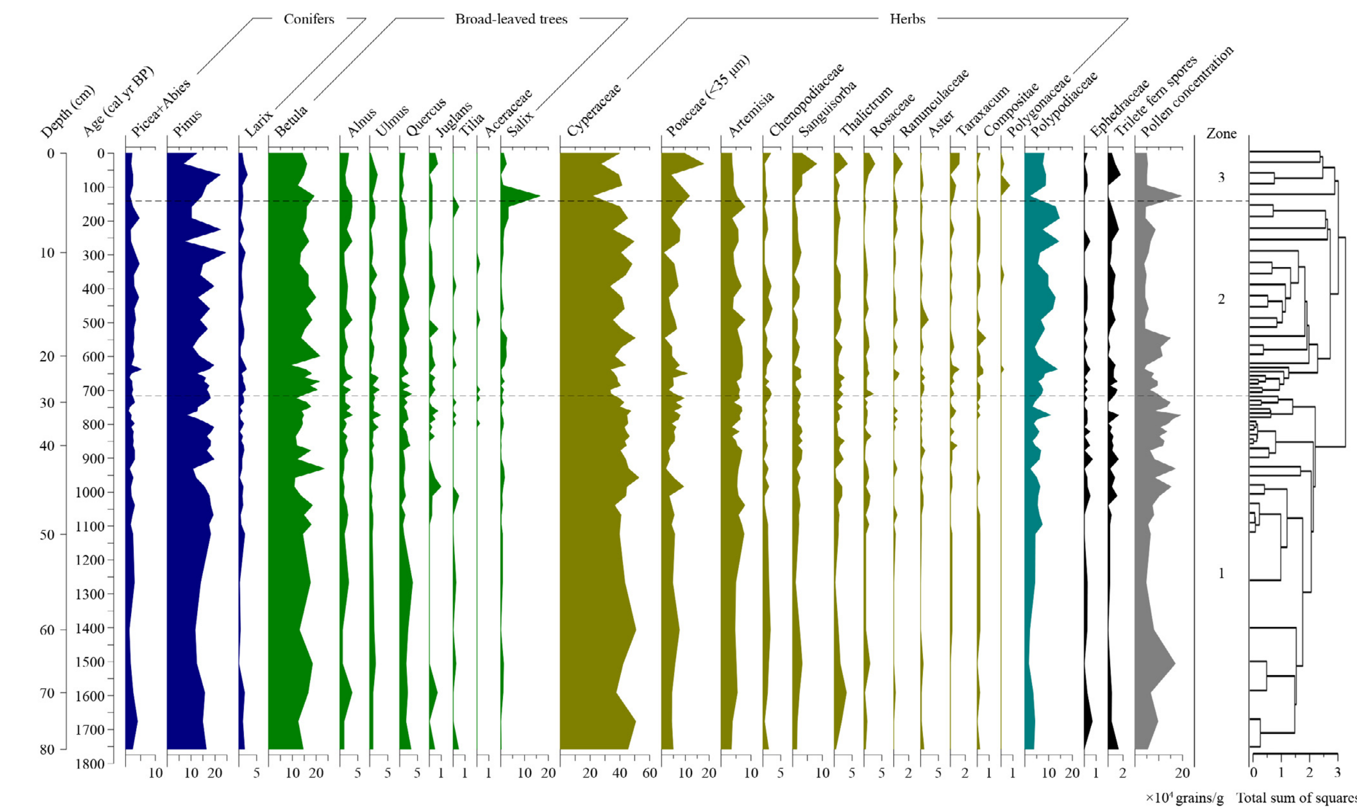

Fig. 3. Pollen percentage diagram of core YH. Zones were identified by CONISS.

1998).

From 150 cal yr BP to present, the percentage of Cyperaceae reduced while the Poaceae (< 35 μm) increased sharply, and the content of *Betula* increased with a decline of *Pinus*, *Picea* and *Abies* (Fig. 3). The increasing broad-leaved trees pollen content and PCA axis 1 score curve both suggested a relatively warm environment, the peat cellulose $\delta^{18}O$ records of Jinchuan peatland marked a warming tendency as well after LIA (Fig. 5). The PCA axis 2 score curve denoted a relatively humid climatic condition. The reconstructed Pann curve in Daihai Lake by Xu et al. (2010) also reflected a higher rainfall compared with LIA, the stalagmite record of Dongge Cave implied a strong East Asian Summer Monsoon intensity, Hulun Lake also recorded a tendency of relative warm and humid climatic condition (Fig. 5).

Overall, we deduced that the dominant species in YH peatland was herbaceous Cyperaceae, with some Poaceae (< 35 μm), *Artemisia*, *Sanguisorba*, *Thalictrum* and Chenopodiaceae, and existed a coniferous and broad-leaved mixed forest (primarily *Pinus* and *Betula*) surrounding the peatland during the last 1750 cal yr BP. The climate changed from

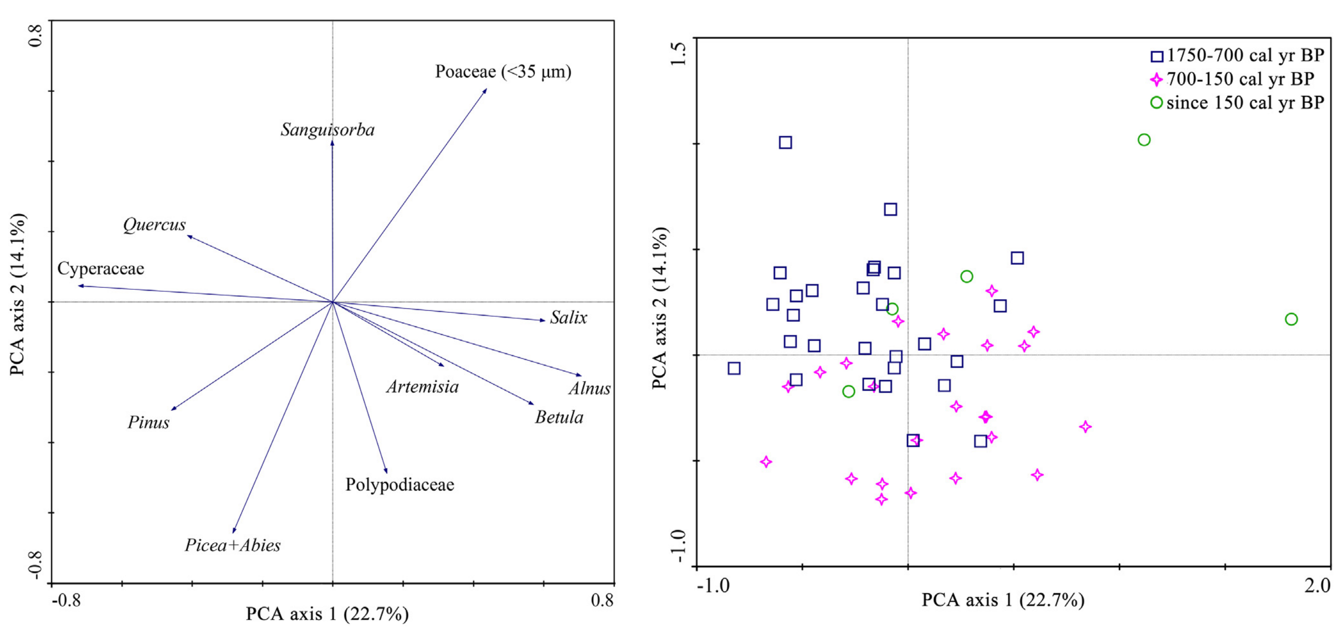

Fig. 4. PCA ordination of principal 11 pollen taxa (left) and samples (right) from YH core.

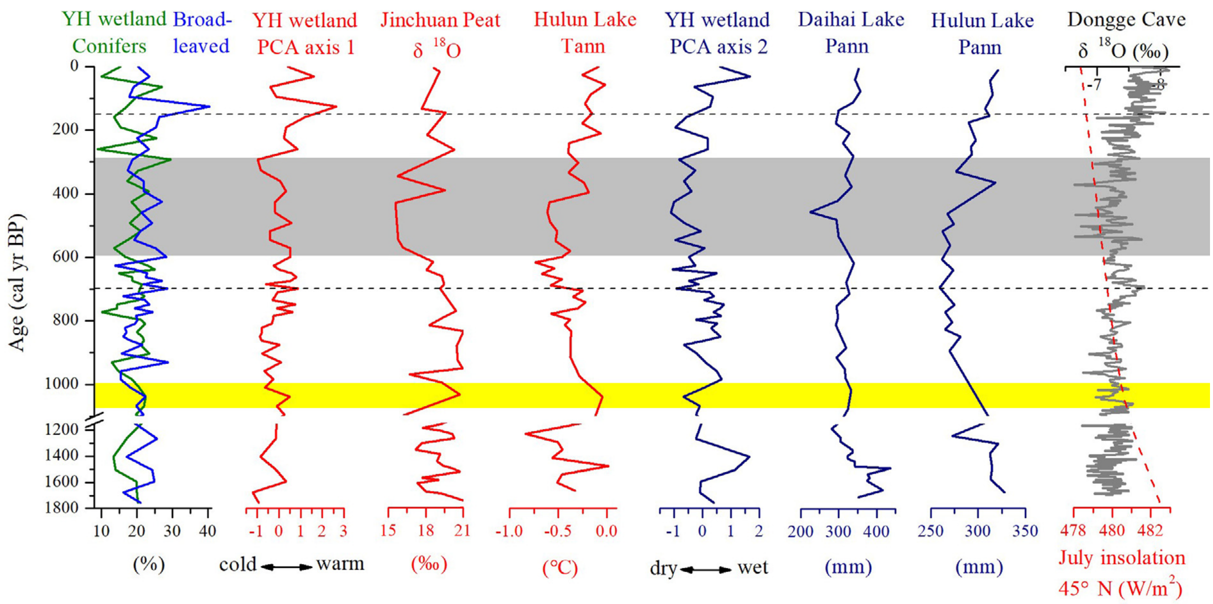

Fig. 5. Comparison of conifers and broad-leaved trees percentages, PCA axis 1 and 2 curves from YH core with other selected proxy records from monsoon region. Tann and Pann of Hulun Lake (Wen et al., 2010a), peat cellulose δ^{18}O of Jinchuan peatland (Hong et al., 2001), Pann of Daihai Lake (Xu et al., 2010), δ^{18}O of Dongge Cave stalagmite (Wang et al., 2005), July insolation at 45° N (Berger and Loutre, 1991). The yellow band marked the time interval of Medieval Warm Period (MWP). The gray band indicated the time interval of Little Ice Age (LIA). Zones derived from fossil pollen data from YH core.

initially moderately cold and wet, to cold and dry, finally warm and moderately humid.

4.2. Spatial differences of vegetation and climate along the Amur River over the last 2000 years

We compared the main pollen assemblages of YH peatland with TQ and HE peatlands during the last 2000 years. As we could see in Fig. 6, there were more arborous trees in the surrounding mountains of TQ peatland in the Greater Khingan Mountains, the percentage of arboreal trees accounted for 68–87% of pollen sum in TQ peatland (Han et al., 2019), was remarkably higher than the other two sites due to its significant elevation above sea level. The predominant species were herbaceous plants in YH peatland in the Lesser Khingan Mountains, the content of Cyperaceae up to 21.5–52.7% in the whole YH core. While there were more hygrophilous taxa in HE peatland in the Sanjiang Plain, mainly included *Equisetum* and Typhacea (Zhang et al., 2015b). We also compared the three peatlands in northeastern China with the adjacent regions from Russian Far East of other researchers, mainly including Ilya floodplain (898 m a.s.l.), which is located at Ilya River, a left tributary of Onon River in the upper Amur River Basin (Bazarova et al., 2008b, 2011), AM23 (126 m a.s.l.) from the mire of Zeysko-Bureinskaya Plains (Yu et al., 2017) in the centre of the Amur River Basin, and Kiya section (100 m a.s.l.) which is situated the southernmost in the lower Amur River Basin (Bazarova et al., 2008a).

From around 2000 to 700 cal yr BP, pollen records investigated *Pinus* was the predominant coniferous tree with some *Abies* and *Picea*, deciduous broad-leaved trees were occupied by *Betula*, *Alnus*, *Quercus* and *Ulmus*, implying there pervasively existed a coniferous and broad-leaved mixed forest (dark coniferous trees dominated, birch trees were subdominant) along the Amur River Basin. Additionally, the herbaceous species in peatlands mainly consisted of Cyperaceae, Poaceae (< 35 μm) and *Artemisia*. The higher Cyperaceae content indicated the climate condition was favorable for the development of peatland. So we speculated the climate was moderately cold and humid at this period.

During the episode of 700–150 cal yr BP, pollen assemblages of TQ peatland exhibited an increasing content of *Larix* (up to 16.5%) and small-shrub (Ericaceae), and a sharp reduction of Cyperaceae (Han et al., 2019). The portion of *Larix* and shrub birch also increased in Ilya floodplain, marking a cooling and strengthening of continental climate (Bazarova et al., 2008b). The percentage of conifers increased, and the broad-leaved trees declined in YH peatland. A substantial decrease of Cyperaceae content also presented in AM23 core, which suggested that the climate was much drier. Additionally, the peak of Ranunculaceae in AM23 core further confirmed the drying condition, as such species flourishing under ephemeral swamp environment (Yu et al., 2017). The proportion of *Pinus* increased and the portion of hygrophilous plants decreased in HE peatland (Zhang et al., 2015b). The declining abundance of broad-leaved *Quercus* and *Ulmus* in Kiya section also revealed a cooling of climate (Bazarova et al., 2008a). All of the above pollen assemblages reflected an increasing content of conifers with a reduction of broad-leaved trees, and a decreasing of Cyperaceae content. The temperature and humidity declined, the climate became colder and drier. The strong climatic cooling and enhanced aridization showed good correspondence with the LIA.

Since about 150 cal yr BP, the content of Cyperaceae declined continuously in YH and HE peatlands, especially in TQ peatland. The decreased content of Cyperaceae suggested the increased aridity and degradation of peatlands. The enhanced aridization also led to the expansion of steppe and the reduction of pine forests in the intracontinental Ilya floodplain (Bazarova et al., 2011).

4.3. Anthropogenic activities along the Amur River Basin

The reconstructed climate based on pollen assemblages was relatively cold in the late Holocene in northeastern China (Wen et al., 2010b; Li et al., 2011). *Pinus* indicated low temperature climate (Yao et al., 2017). Wen et al. (2010b) also demonstrated pine forests expanded when the temperature dropped in the Hulun Lake region. During this cold period, the sharp reduction of *Pinus* species was illogical in HE peatland since around 1800 cal yr BP especially since 1300 cal yr BP and in TQ peatland at about 600 cal yr BP, respectively. Hence, we speculated the climatic variability was not the only driving force of vegetation change, anthropogenic activities (human occupation and agricultural activities) also influenced the local ecosystem. In HE peatland, the content of *Pinus* declined sharply at around 1800 cal yr BP, especially since about 1300 cal yr BP (Fig. 6). At the era of disunity (220–580 CE, 1730–1370 cal yr BP), the frequency of armed conflicts

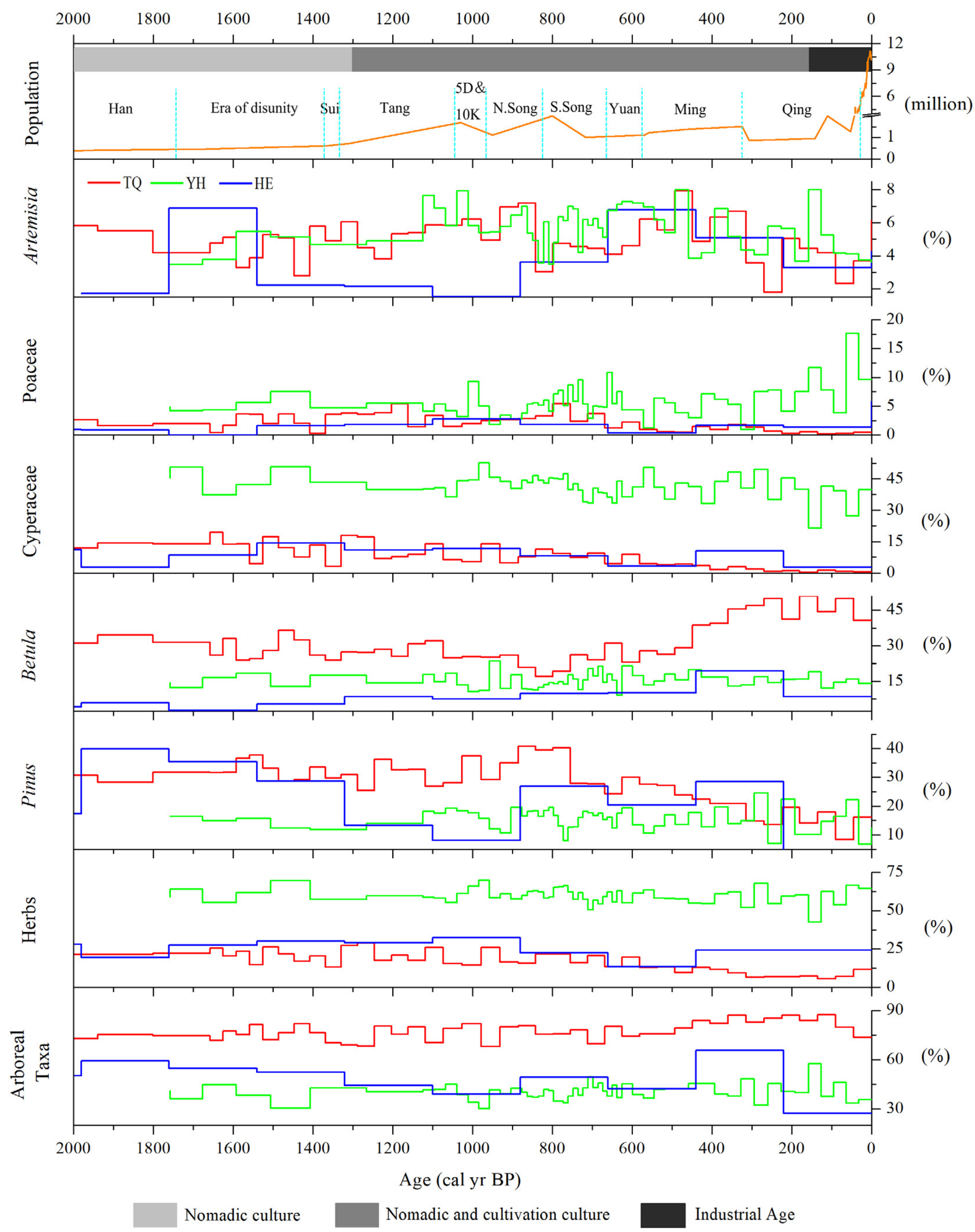

Fig. 6. Pollen percentages of arboreal and herbaceous taxa, selected main pollen proportions of *Pinus*, *Betula*, Cyperaceae, Poaceae (< 35 μm) and *Artemisia* along the Amur River Basin since 2000 cal yr BP. The historical population of Heilongjiang Province (Cong et al., 2016) was included. 5D & 10 K represented the period of Five Dynasties and Ten Kingdoms in China.

was higher, the wars and fires led to a reduction of pine forest directly. As we know, the rainfall and temperature gradually increased from the upstream to downstream along the Amur River Basin (Bazarova et al., 2011; Yu et al., 2014; Yang et al., 2015), the river plain was fertile and suitable for human occupation and agricultural activities in the Sanjiang Plain. Usually, people cleared vegetation and developed lands to meet their daily needs when migrated to a new area. An increasing of Heilongjiang Province population occurred with the foundation of Tang Dynasty (618–907 CE, 1332–1043 cal yr BP). People felled trees, opened lands for building settlements and began to reclaim the cultivated lands in the Sanjiang Plain, the content of *Pinus* decreased obviously at approximately 1300 cal yr BP. Charcoal records in the Jinchuan peatland (south of the Sanjiang Plain) also showed that the spread of the Han farming culture accompanied by the territorial expansion of the Tang Dynasty to Sanjiang Plain at approximately 1288 cal yr BP (Jiang et al., 2008). Likewise, a selective lumbering occurred in TQ peatland in Greater Khingan Mountains since about 600 cal yr BP, people used woods to build houses and make fires during the LIA, meanwhile, logging led to the expansion of secondary birch forests (Li et al., 2011; Mackenzie et al., 2018). The increasing contents of pollen indicators of human activities, including weeds and cereal Poaceae, Polygonaceae, *Taraxacum*, *Artemisia*, *Asteraceae* and other Compositae species, could suggest the intensification of anthropogenic activities (Zhang et al. 2015c; Li et al., 2015). Since about 800 cal yr BP (at the depth of 34 cm in YH core), cereal Poaceae (> 35 μm) occurred, indicating human activities of cultivation in the Lesser Khingan

Mountains. Additionally, as we could see in Fig. 6, the content of *Aster*, *Taraxacum* and Polygonaceae (human-companion plants) increased, indicating intensified human activities since 800 cal yr BP. Meanwhile there was an increase of the population in Heilongjiang Province at Yuan and Ming Dynasty (Fig. 6).

It has been documented that a major increase in immigration took place with the foundation of the Qing Dynasty (1616–1912 CE, 334–38 cal yr BP) in northeastern China (Northeast Culture Community, 1931; Mackenzie et al., 2018). The population of Heilongjiang Province sharply increased to several millions within the last 150 years (Fig. 6), human beings disturbed the ecosystem and natural environment seriously by deforestation, land-reclamation and agricultural activities. The pollen and charcoal records along the Amur River Basin registered the expansion of population in this period. Zhang et al. (2015b) attributed the frequent fires to intensified human influence with the obviously increased population and land use in the Sanjiang Plain since 300 cal yr BP. Yu et al. (2017) deduced the significant increase of charcoal concentration and expansion of secondary forests at about 250 cal yr BP likely caused by the anthropogenic fires in AM23 core in the far-eastern Russia. The continuous reduction of pines and the expansion of birches indicating a clearly intensification of human influence since 300 cal yr BP (Han et al., 2019). Furthermore, the obviously increasing proportions of human-companion plants, such as weeds Poaceae (< 35 μm), *Taraxacum*, Ranunculaceae and Polygonaceae in YH peatland also indicated the intensification of anthropogenic activities in the recent 150 years.

In short, we presumed that the human agricultural activities occurred earlier in the Sanjiang Plain since around 1300 cal yr BP, while the agricultural activities in the Lesser Khingan Mountains were relatively later, at approximately 800 cal yr BP. The human disturbance in the Greater Khingan Mountains mainly by logging since about 600 cal yr BP. An obvious intensification of anthropogenic activities occurred in recent 150 years along the Amur River Basin.

5. Conclusions

The pollen assemblages revealed the past vegetation and climate during the past 2000 years along the Amur River Basin. There was a synchrony of vegetation change along the Amur River Basin during the late Holocene. During the period of 2000–700 cal yr BP, the basin was inhabited mainly by the coniferous and broad-leaved mixed forest, peatland vegetation was occupied by Cyperaceae, the climate was moderately cold and wet. The interval from 700 to 150 cal yr BP, responded to Little Ice Age, the cold and dry climate conditions resulted in the expansion of coniferous forests and a reduction of broad-leaved trees and Cyperaceae content. Since about 150 cal yr BP, the climate tended to be moderately warm, intensified anthropogenic activities led to the enlargement of secondary forests and a continuously reduction of Cyperaceae. Additionally, early human occupation (felling and planting) occurred approximately at 1300 cal yr BP in the Sanjiang Plain. People began to cultivate at about 800 cal yr BP in the Lesser Khingan Mountains and to log pine trees at around 600 cal yr BP in the Greater Khingan Mountains. Human influence on peatland vegetation variability intensified rapidly in the recent 150 years along the Amur River Bain.

Declaration of Competing Interest

The authors declare that they have no known competing financial interests or personal relationships that could have appeared to influence the work reported in this paper.

Acknowledgements

The authors gratefully acknowledge the assistance of the Analysis and Test Center of the Northeast Institute of Geography and Agroecology of the Chinese Academy of Sciences. Special thanks are entended to Dr. Wei Xing for his valuable discussions and suggestions. We also thank Christopher R. Bryant and two anonymous reviewers for their constructive comments and suggestions to improve the quality of this manuscript. This work was supported by the National Key Research and Development Project (No. 2016YFA0602301), the National Natural Science Foundation of China (No. 41701217, 41571191), the Youth Innovation Promotion Association CAS (No. 2020235), the Fundamental Research Funds for the Central Universities (No. 2412019BJ003), and the Jilin Provincial Department of Science and Technology (No. 20190101011JH).

References

Bao, K.S., Xing, W., Song, L.H., Li, H.K., Liu, H.X., Wang, G.P., 2018. A 100-year history of water level change and driving mechanism in Heilongjiang River basin wetlands. Quaternary Sci. 38 (4), 981–995 (In Chinese with English abstract).

Bazarova, V.B., Klimin, M.A., Mokhova, L.M., Orlova, L.A., 2008a. New pollen records of Late Pleistocene and Holocene changes of environment and climate in the Lower Amur River basin, NE Eurasia. Quat. Int. 179 (1), 9–19.

Bazarova, V.B., Mokhova, L.M., Klimin, M.A., Orlova, L.A., Bazarov, K.Y., 2008b. Climatic changes and alluvial-sedimentation settings in southeastern Transbaikalia in the Middle-Late Holocene (*by the example of the Ilya floodplain*). Russ. Geol. Geophys. 49 (12), 978–985.

Bazarova, V.B., Mokhova, L.M., Klimin, M.A., Kopoteva, T.A., 2011. Vegetation development and correlation of Holocene events in the Amur River basin, NE Eurasia. Quat. Int. 237 (1), 83–92.

Berger, A.L., Loutre, M.F., 1991. Insolation values for last 10 million years. Quat. Sci. Rev. 10 (4), 297–317.

Blaauw, M., Christen, J.A., 2011. Flexible paleoclimate age-depth models using an autoregressive gamma process. Bayesian Anal. 6 (3), 457–474.

Birks, H.J.B., Gordon, A.D., 1985. Numerical Methods in Quaternary Analysis. Academic Press, London.

Borren, W., Bleuten, W., Lapshina, E.D., 2004. Holocene peat and carbon accumulation rates in the southern taiga of western Siberia. Quat. Res. 61, 42–51.

Cai, S.S., Yu, Z.C., 2011. Response of a warm temperate peatland to Holocene climate change in northeastern Pennsylvania. Quat. Res. 75, 531–540.

Chen, X.M., Chen, F.H., Zhou, A.F., Huang, X.Z., Tang, L.Y., Wu, D., Zhang, X.J., Yu, J.Q., 2014. Vegetation history, climate changes and Indian summer monsoon evolution during the last glaciation (36,400–13,400 cal yr BP) documented by sediments from Xingyun Lake, Yunnan, China. Palaeogeogr. Palaeoclimatol. Palaeoecol. 410 (5), 179–189.

Chu, G.Q., Sun, Q., Xie, M.M., Lin, Y., Shang, W.Y., Zhu, Q.Z., Shan, Y.B., Xu, D.K., Rioual, P., Wang, L., Liu, J.Q., 2014. Holocene cyclic climatic variations and the role of the Pacific Ocean as recorded in varved sediments from northeastern China. Quat. Sci. Rev. 102, 85–95.

Cong, J.X., Gao, C.Y., Zhang, Y., Zhang, S.Q., He, J.B., Wang, G.P., 2016. Dating the period when intensive anthropogenic activity began to influence the Sanjiang Plain, Northeast China. Sci. Rep. 6, 22153.

Core Team, R., 2015. R: A Language and Environment for Statistical Computing. R Foundation for Statistical Computing, Vienna, Austria.

Dai, C.L., Wang, S.C., Li, Z.J., Zhang, Y.D., Gao, Y., Li, C., 2015. Review on hydrological geography in Heilongjiang River Basin. Acta Geographica Sinica 70 (11), 1823–1834 (In Chinese with English abstract).

Fægri, K., Iversen, J., 1989. Textbook of Pollen Analysis, 4th ed. John Wiley and Sons, London, UK.

Han, D.X., Gao, C.Y., Yu, Z.C., Yu, X.F., Li, Y.H., Cong, J.X., Wang, G.P., 2019. Late Holocene vegetation and climate changes in the Great Hinggan Mountains, Northeast China. Quat. Int. 532, 138–145.

Herzschuh, U., Kürschner, H., Mischke, S., 2006. Temperature variability and vertical vegetation belt shifts during the last ~50,000 yr in the Qilian Mountains (NE margin of the Tibetan Plateau, China). Quat. Res. 66 (1), 133–146.

Hong, Y.T., Wang, Z.G., Jiang, H.B., Lin, Q.H., Hong, B., Zhu, Y.X., Wang, Y., Xu, L.S., Leng, X.T., Li, H.D., 2001. A 6000-year record of changes in drought and precipitation in northeastern China based on a $\delta^{13}C$ time series from peat cellulose. Earth Planet. Sci. Lett. 185 (1), 111–119.

IPCC, 2013. Summary for policymakers. In: Stocker, T.F., Qin, D., Plattner, G.-K., Tignor, M., Allen, S.K., Boschung, J., Nauels, A., Xia, Y., Bex, V., Midgley, P.M. (Eds.), Climate Change 2013: the Physical Science Basis. Contribution of Working Group I to the Fifth Assessment Report of the Intergovernmental Panel on Climate Change. Cambridge University Press, Cambridge, United Kingdom and New York, NY, USA.

Jiang, W.Y., Leroy, S.A.G., Ogle, N., Chu, G.Q., Wang, L., Liu, J.Q., 2008. Natural and anthropogenic forest fires recorded in the Holocene pollen record from a Jinchuan peat bog, northeastern China. Palaeogeogr. Palaeocl. 261 (1), 47–57.

Lamb, H.H., 1972. The Cold Little Ice Age Climate of about 1550 to 1800. In: Climate: Present, Past and Future. Methuen, London.

Lamentowicz, M., Gałka, M., Lamentowicz, Ł., Obremska, M., Kühl, N., Lücke, A., Jassey, V.E.J., 2015. Reconstructing climate change and ombrotrophic bog development during the last 4000 years in northern Poland using biotic proxies, stable isotopes and trait-based approach. Palaeogeogr. Palaeoclimatol. Palaeoecol. 418, 261–277.

Li, C.H., Wu, Y.H., Hou, X.H., 2011. Holocene vegetation and climate in Northeast China revealed from Jingbo Lake sediment. Quat. Int. 229 (1), 67–73.
Li, M.Y., Xu, Q.H., Zhang, S.R., Li, Y.C., Ding, W., Li, J.Y., 2015. Indicator pollen taxa of human-induced and natural vegetation in Northern China. Holocene 25 (4), 686–701.
Liu, H.X., Gao, C.Y., Wei, C.F., Wang, C.L., Yu, X.F., Wang, G.P., 2018. Evaluating the timing of the start of the Anthropocene from Northeast China: Applications of stratigraphic indicators. Ecol. Indic. 84 (84), 738–747.
Mackenzie, L., Bao, K.S., Mao, L.M., Klamt, A.M., Pratte, S., Shen, J., 2018. Anthropogenic and climate-driven environmental change in the Songnen Plain of northeastern China over the past 200 years. Palaeogeogr. Palaeoclimatol. Palaeoecol. 1–10.
Mann, M.E., Bradley, R.S., Hughes, M.K., 1998. Global-scale temperature patterns and climate forcing over the past six centuries. Nature 392, 779–787.
Melles, M., Svendsen, J.I., Fedorov, G., Wagner, B., 2019. Northern Eurasian lakes-late Quaternary glaciation and climate history-introduction. Boreas 48, 269–272.
Northeast Culture Community, 1931. The Yearbooks of Northeastern China. pp. 97-269.
Novorotskii, P.V., 2007. Climate Changes in the Amur River Basin in the Last 115 Years. Russ. Meteorol. Hydrol. 32 (2), 102–109.
Reimer, P.J., Bard, E., Bayliss, A., Beck, J.W., Blackwell, P.G., Ramsey, C.B., Buck, C.E., Cheng, H., Edwards, R.L., Friedrich, M., 2013. Intcal 13 and marine 13 radiocarbon age calibration curves 0–50,000 years cal BP. Radiocarbon 55, 1869–1887.
Schellekens, J., Buurman, P., Fraga, I., Martinez-Cortizas, A., 2011. Holocene vegetation and hydrologic changes inferred from molecular vegetation markers in peat, Penido Vello (Galicia, Spain). Palaeogeogr. Palaeoclimatol. Palaeoecol. 299, 56–69.
Stebich, M., Rehfeld, K., Schlütz, F., Tarasov, P.E., Liu, J.Q., Mingram, J., 2015. Holocene vegetation and climate dynamics of NE China based on the pollen record from Sihailongwan Maar Lake. Quat. Sci. Rev. 124, 275–289.
Tang, L.Y., Mao, L.M., Shu, J.W., Li, C.H., Shen, C.M., Zhou, Z.Z., 2016. An Illustrated Handbook of Quaternary Pollen and Spores in China. Science Press, Beijing (In Chinese).
TerBraak, C.J.F., Smilauer, P., 2003. CANOCO Reference Manual and CanoDraw for Windows User's Guide: Software for Canonical Community Ordination (Version 4.5). Microcomputer Power, Ithaca, NY.
Wang, C.L., Zhao, H.Y., Wang, G.P., 2015. Vegetation development and water level changes in Shenjiadian peatland in Sanjiang Plain, Northeast China. Chin. Geogr. Sci. 25 (4), 451–461.
Wang, F.X., Qian, N.F., Zhang, Y.L., Yang, H.Q., 1995. Pollen Flora of China. Science Press, Beijing (In Chinese).
Wang, Y.J., Cheng, H., Edwards, R.L., He, Y.Q., Kong, X.G., An, Z.S., Wu, J.Y., Kelly, M.J., Dykoski, C.A., Li, X.D., 2005. The Holocene Asian monsoon: links to solar changes and North Atlantic climate. Science 308, 854–856.
Wen, R.L., Xiao, J.L., Chang, Z.G., Zhai, D.Y., Xu, Q.H., Li, Y.C., Itoh, S., 2010a. Holocene precipitation and temperature variations in the East Asian monsoonal margin from pollen data from Hulun Lake in northeastern Inner Mongolia, China. Boreas 39 (2), 262–272.
Wen, R.L., Xiao, J.L., Chang, Z.G., Zhai, D.Y., Xu, Q.H., Li, Y.C., Itoh, S., Lomtatidze, Z., 2010b. Holocene climate changes in the mid-high-latitude-monsoon margin reflected by the pollen record from Hulun Lake, northeastern Inner Mongolia. Quat. Res. 73 (2), 293–303.
Wen, R.L., Xiao, J.L., Fan, J.W., Zhang, S.R., Yamagata, H., 2017. Pollen evidence for a mid-Holocene East Asian summer monsoon maximum in northern China. Quat. Sci. Rev. 176, 29–35.
Wu, J., Liu, Q., Wang, L., Chu, G.Q., Liu, J.Q., 2016. Vegetation and climate change during the Last Deglaciation in the Great Khingan Mountain, Northeastern China. PLoS ONE 11 (1), 1–16.
Xiao, J.L., Xu, Q.H., Nakamura, T., Yang, X.L., Liang, W.D., Inouchi, Y., 2004. Holocene vegetation variation in the Daihai Lake region of north-central China: a direct indication of the Asian monsoon climatic history. Quat. Sci. Rev. 23 (14), 1669–1679.
Xing, W., Bao, K.S., Gallego-Sala, A.V., Charman, D.J., Zhang, Z.Q., Gao, C.Y., Lu, X.G., Wang, G.P., 2015. Climate controls on carbon accumulation in peatlands of Northeast China. Quat. Sci. Rev. 115 (9), 78–88.
Xu, Q.H., Chen, F.H., Zhang, S.R., Cao, X.Y., Li, J.Y., Li, Y.C., Li, M.Y., Chen, J.H., Liu, J.B., Wang, Z.L., 2016. Vegetation succession and East Asian Summer Monsoon Changes since the last deglaciation inferred from high-resolution pollen record in Gonghai Lake, Shanxi Province, China. Holocene 27 (6), 835–846.
Xu, Q.H., Xiao, J.L., Li, Y.C., Tian, F., Nakagawa, T., 2010. Pollen-based quantitative reconstruction of Holocene climate changes in the Daihai Lake area, Inner Mongolia, China. J. Climate 23 (11), 2856–2868.
Yang, W., Zhang, S.W., Jiang, X.L., 2015. Burned area mapping for Heilongjiang basin based on MODIS time series data. Acta Ecol. Sinica 35 (17), 5866–5873 (In Chinese with English abstract).
Yang, Y.X., Wang, S.Y., 2002. Study on mire development and palaeoenvironment change since 9.0 ka B.P. in the east part of the Xiaoxinganling Mountains. Journal of Mountain Science 20 (2), 129-134 (In Chinese with English abstract).
Yao, F.L., Ma, C.M., Zhu, C., Li, J.Y., Chen, G., Tang, L.Y., Huang, M., Jia, T.J., Xu, J.J., 2017. Holocene climate change in the western part of Taihu Lake region, East China. Palaeogeogr. Palaeoclimatol. Palaeoecol. 485, 963–973.
Yu, L.X., Zhang, S.W., Guan, C., Yan, F.Q., Yang, C.B., Bu, K., Yang, J.C., Chang, L.P., 2014. Monitoring on spatial and temporal changes of snow cover in the Heilongjiang Basin based on remote sensing. Chin. J. Appl. Ecol. 25 (9), 2521–2528 (In Chinese with English abstract).
Yu, S.H., Zheng, Z., Kershaw, P., Skrypnikova, M., Huang, K.Y., 2017. A late Holocene record of vegetation and fire from the Amur Basin, far-eastern Russia. Quat. Int. 432, 79–92.
Yu, Z.C., Beilman, D.W., Jones, M.C., 2009. Sensitivity of northern peatland carbon dynamics to Holocene climate change. Carbon Cycling in Northern Peatlands Geophysical Monograph Series 184, 55–67.
Yu, Z.C., Loisel, J., Brosseau, D.P., Beilman, D.W., Hunt, S.J., 2010. Global peatland dynamics since the Last Glacial Maximum. Geophys. Res. Lett. 37 (L13402).
Zhang, H., Piilo, S.R., Amesbury, M.J., Charman, D.J., Gallego-Sala, A.V., Väliranta, M.M., 2018a. The role of climate change in regulating arctic permafrost peatland hydrological and vegetation change over the last millennium. Quat. Sci. Rev. 182, 121–130.
Zhang, H., Zhang, Y., Kong, Z.C., Yang, Z.J., Li, Y.M., Tarasov, P.E., 2015a. Late Holocene climate change and anthropogenic activities in north Xinjiang: Evidence from a peatland archive, the Caotanhu wetland. Holocene 25 (2), 323–332.
Zhang, Y., Meyers, P.A., Liu, X.T., Wang, G.P., Ma, X.H., Li, X.Y., Yuan, Y.X., Wen, B.L., 2016. Holocene climate changes in the central Asia mountain region inferred from a peat sequence from the Altai Mountains, Xinjiang, northwestern China. Quat. Sci. Rev. 152, 19–30.
Zhang, Z.Q., Xing, W., Wang, G.P., Tong, S.Z., Lv, X.G., Sun, J.M., 2015b. The peatlands developing history in the Sanjiang Plain, NE China, and its response to East Asian monsoon variation. Sci. Rep. 5 (5), 11316.
Zhang, Z.Q., Yao, Q., Bianchette, T.A., Liu, K.B., Wang, G.P., 2018b. A multi-proxy quantitative record of Holocene hydrological regime on the Heixiazi Island (NE China): indications for the evolution of East Asian summer monsoon. Clim. Dyn. 1–14.
Zhang, Z.Q., Zhong, J.J., Lv, X.G., Tong, S.Z., Wang, G.P., 2015c. Climate, vegetation and human influences on late-Holocene fire regimes in the Sanjiang Plain, northeastern China. Palaeogeogr. Palaeoclimatol. Palaeoecol. 438, 1–8.
Zhao, C., Li, X.Q., Zhou, X.Y., Zhao, K.L., Yang, Q., 2015. Holocene vegetation succession and response to climate change on the south bank of the Heilongjiang-Amur River, Mohe County, Northeast China. Adv. Meteorol. 2016 (12), 1–11.
Zhao, Y., Yu, Z.C., Liu, X.J., Zhao, C., Chen, F.H., Zhang, K., 2010. Late Holocene vegetation and climate oscillations in the Qaidam Basin of the northeastern Tibetan Plateau. Quat. Res. 73 (1), 59–69.